JOURNAL OF Materials CHEMISTRY

Preparation and characterization of phthalocyanine-based organic alloy $Co_xNi_{1-x}Pc(AsF_6)_{0.5}$ ($0 \leqslant x \leqslant 1$)

Yuqin Ding, Mkhital Simonyan, Yukako Yonehara, Mikio Uruichi and Kyuya Yakushi*

Institute for Molecular Science and Graduate University for Advanced Studies, Myodaiji, Okazaki 444-8585, Japan. E-mail: yakushi@ims.ac.jp; Fax: 81-564-54-2254

Received 2nd January 2001, Accepted 13th February 2001
First published as an Advance Article on the web 13th March 2001

The organic alloy, $Co_xNi_{1-x}Pc(AsF_6)_{0.5}$ ($0<x<1$), was prepared and characterized by elementary analysis (EPMA), X-ray diffraction, ESR, magnetic susceptibility, Raman spectroscopy and reflection spectroscopy. These experiments show that mixed crystals are formed for a wide range of x although $CoPc(AsF_6)_{0.5}$ is not exactly isomorphous to $NiPc(AsF_6)_{0.5}$. The mixing on a molecular level is proved by the x dependence of the ESR and Raman spectra over the whole range of x. Based on these results combined with the reflectivity spectra, we propose a model for the energy band near the Fermi level including the 3d bands. This band model explains the differences in the magnetic and optical properties between $CoPc(AsF_6)_{0.5}$ and $NiPc(AsF_6)_{0.5}$.

Introduction

The quasi-one-dimensional phthalocyanine conductors $MPc(X)_y$ ($M=H_2^{2+}$, Co^{2+}, Ni^{2+}, Cu^{2+}; $Pc=(C_{32}N_8H_{16})^{2-}$; $y=0.5$ for $X=AsF_6^-$, $y=0.33$ for I_3^-) consist of metal and macrocycle (Pc) chains running parallel to each other. Since the molecules are stacked in a metal-over-metal fashion, the one-dimensional (1D) metal chain is surrounded with the 1D macrocycle chain. Owing to their orbital symmetry, the 3d orbitals except for $3d_{xz}$ and $3d_{yz}$ are not hybridized with the $2p_z$ orbital of Pc, and thus preserve independent d-character. The π electrons are not only delocalized within the macrocycle but also extended to the neighboring molecules, whereas 3d electrons are localized near the central metal. Because of the structural characteristics, phthalocyanine conductors show π- and d-character in their solid state properties. The effect of the 3d orbital becomes obvious, particularly when the 3d orbital of the central metal is singly occupied such as in paramagnetic CuPc and CoPc. Both the paramagnetic ($M=Co^{2+}$, Cu^{2+}) and diamagnetic ($M=H_2^{2+}$, Ni^{2+}) phthalocyanines yield nearly isostructural metallic charge-transfer salts. Accordingly, a comparative study of the phthalocyanine-based conductors with paramagnetic and diamagnetic molecules and their alloys has been conducted in order to elucidate the role of the singly occupied 3d electrons. Ogawa *et al.* suggested a strong coupling between the localized spin of Cu^{2+} ($S=1/2$) and the conduction electron of the Pc chain in $CuPc(I_3)_{0.33}$.[1,2] The influence of the localized spin of Cu^{2+} on the conductivity was studied by Quirion *et al.* on $CuPc(I_3)_{0.33}$ and analogous compounds, in which in a microwave resistivity experiment they found a huge negative magneto-resistance and proposed a spin-flip scattering process produced by Cu^{2+} local spin.[3,4] They studied the alloys with diamagnetic phthalocyanine molecules, $Cu_xNi_{1-x}Pc(I_3)_{0.33}$[5,6] and $Cu_xH_{2(1-x)}Pc(I_3)_{0.33}$[7] as well. Martinsen *et al.* reported the phthalocyanine conductor of another paramagnetic ion, Co^{2+} ($S=1/2$), on $CoPc(I_3)_{0.33}$, in which the central metal spine was responsible for the conductivity.[8] The authors reported a similar Co-containing phthalocyanine conductor $CoPc(AsF_6)_{0.5}$.[9] In contrast to $CoPc(I_3)_{0.33}$, the Pc chain played a part in the electrical conductivity, and thus the Co^{2+} ions were anticipated to play the same role as Cu^{2+} in $CuPc(I_3)_{0.33}$. However, the singly occupied molecular orbital (SOMO) of Co^{2+} is different from that of Cu^{2+}. Owing to the difference in SOMO, the magnetic and optical properties are different from each other. For example, the spin susceptibility Co^{2+} is very suppressed in $CoPc(AsF_6)_{0.5}$,[10] whereas the Cu^{2+} spin of $CuPc(I_3)_{0.33}$ is nearly free from antiferromagnetic interaction.[2] The plasma edge of $CoPc(AsF_6)_{0.5}$ appears at significantly higher energy than that of $CuPc(I_3)_{0.33}$.[2,10] To elucidate the role of the 3d orbital of Co^{2+} in $CoPc(AsF_6)_{0.5}$, we prepared alloys containing $NiPc(AsF_6)_{0.5}$. In this paper, we characterize the alloy $Co_xNi_{1-x}Pc(AsF_6)_{0.5}$ by means of elemental analysis, crystal structure analysis, ESR, magnetic susceptibility, Raman spectroscopy, and reflection spectroscopy, and present a band model near the Fermi level.

Experimental

The single crystals of $Co_xNi_{1-x}Pc(AsF_6)_{0.5}$ were grown electrochemically in 1-chloronaphthalene solution.[11] For the preparation of $Co_xNi_{1-x}Pc(AsF_6)_{0.5}$, crystals of crude phthalocyanines CoPc and NiPc were carefully weighed and ground together with corresponding weighting factors (NiPc : CoPc = 100 : 1, 50 : 1, 10 : 1, *etc.*). The mixtures were sublimed four times under a high vacuum to ensure intimate mixing. After allowing the electrochemical reaction to proceed for three weeks, all the starting materials were transformed into the AsF_6 salts. The atomic ratio between Ni and Co in the $Co_xNi_{1-x}Pc(AsF_6)_{0.5}$ single crystals was determined on an EPMA system (Hitachi S-450). Kovar (alloy consisting of Co, Ni and Fe as main components), $CoPc(AsF_6)_{0.5}$, and $NiPc(AsF_6)_{0.5}$ were used as the standards for the analysis of cobalt and nickel concentrations. The analysis of several points on each single crystal indicated that the distribution of Co and Ni atoms in the samples was homogeneous. In all cases, the Co to Ni ratio in several crystals agreed with each other within 10%. The X-ray diffraction data were collected on an imaging-plate diffractometer (Rigaku R-AXIS-IV) using a dark purple crystal with a needle-like shape. The linear absorption coefficients are μ(Mo-Kα) = 1.43 mm^{-1} and 1.36 mm^{-1} for crystals with $x=0.25$ and 0.45. The 388 and 70 parameters were refined by full-matrix least-squares methods using 1739 and 436 independent reflections with $I>3\sigma(I)$ for $x=0.25$ and $x=0.45$, respectively. ESR measurements were carried out on an ESR spectrometer with an X-band cavity (Bruker ESP-300E). The temperature was controlled within ± 0.1 K using a helium-gas

DOI: 10.1039/b100043h

Table 1 Lattice parameters of $Co_xNi_{1-x}Pc(AsF_6)_{0.5}$

	$NiPc(AsF_6)_{0.5}$	$Co_{0.25}Ni_{0.75}Pc(AsF_6)_{0.5}$	$Co_{0.45}Ni_{0.55}Pc(AsF_6)_{0.5}$	$CoPc(AsF_6)_{0.5}$
Formula	$C_{32}H_{16}N_8NiAs_{0.5}F_3$	$C_{32}H_{16}N_8Co_{0.25}Ni_{0.75}As_{0.5}F_3$	$C_{32}H_{16}N_8Co_{0.45}Ni_{0.55}As_{0.5}F_3$	$C_{32}H_{16}N_8CoAs_{0.5}F_3$
Formula weight	665.7	665.8	665.8	665.9
Crystal class	orthorhombic	orthorhombic	tetragonal	tetragonal
Space group	*Pnc*2	*Pnc*2	*P*4/*mcc*	*P*4/*mcc*
a/Å	14.015(1)	14.033(4)	14.226(2)	14.234(2)
b/Å	28.485(2)	28.54(1)	14.226(2)	14.234(2)
c/Å	6.466(3)	6.435(2)	6.414(1)	6.296(2)
V/Å^3	2581(1)	2577(2)	1298.1(3)	1275.6(4)
Z	4	4	2	2
R-factor	6.5%	6.8%	7.0%	7.3%
	ref. 12	this work	this work	ref. 10

flow-type cryostat (Oxford ESR-900 and ITC-4). For the angular dependent ESR experiment, aligned single crystals were mounted on a quartz rod. The static magnetic susceptibility was measured on a SQUID magnetometer (Quantum Design MPMS 7000). About 1 mg of single crystals was aligned on a quartz plate to detect anisotropy. The Raman spectrum was measured on a micro-Raman spectrometer (Renishaw Ramascope System-1000) with a back-scattering geometry. The numerical aperture of the objective lens of the microscope was 0.42, in which the maximum incident angle was 25°. The scattered light was analyzed using a polarization filter with an extinction ratio of 10^{-4}. For example, the (c,a) spectrum denotes an experimental condition in which the laser is polarized along the *c*-axis, and the analyzer is polarized along the *a*-axis. A He–Ne laser (633 nm) and an Ar^+ laser (515 nm) were employed as excitation sources. The laser power was reduced by a neutral filter to 0.2 mW. The polarized reflection spectrum was obtained using two spectrometers and a microscope (Spectratech IR-Plan). A Nicolet Magna 760 FT-IR spectrometer was used for the 600–12000 cm^{-1} region and an Atago Macs320 multi-channel detection system was used for the 11000–30000 cm^{-1} region. The reflectivity in the far-infrared region, 50–700 cm^{-1}, was measured on a Bruker IFS-113v FT-IR spectrometer using aligned mosaic crystals.

Results and discussion

Crystal structure

The elementary analysis by means of EPMA suggested that $NiPc(AsF_6)_{0.5}$ and $CoPc(AsF_6)_{0.5}$ formed the alloy $Co_xNi_{1-x}Pc(AsF_6)_{0.5}$ in a wide range of *x*. Fig. 1 shows the crystal structures of $Co_xNi_{1-x}Pc(AsF_6)_{0.5}$ with $x=0.25$ and 0.45 viewed along the stacking axis. The structure was solved using the occupancy factors of Ni and Co determined by EPMA. Owing to the high symmetry of the $CoPc(AsF_6)_{0.5}$ crystal, AsF_6^- is orientationally disordered. The lattice parameters are listed in Table 1 along with those of $NiPc(AsF_6)_{0.5}$ ($x=0$)[12] and $CoPc(AsF_6)_{0.5}$ ($x=1$).[10] The boundary of the tetragonal and orthorhombic systems is located between $x=0.25$ and 0.45 in this alloy system. The unit cell of $NiPc(AsF_6)_{0.5}$ involves two conducting columns with a metal-over-metal stack, half of the unit cell being almost the same as the unit cell of $CoPc(AsF_6)_{0.5}$. Therefore the structure of $CoPc(AsF_6)_{0.5}$ is nearly isostructural to $NiPc(AsF_6)_{0.5}$, which is considered as the reason for the formation of the mixed crystal system over a wide range of *x*. A significant difference exists in the *c*-axes between $NiPc(AsF_6)_{0.5}$ and $CoPc(AsF_6)_{0.5}$. This difference is explained by the doubly occupied $3d_{z^2}$ orbital in NiPc and singly occupied $3d_{z^2}$ orbital in CoPc.[10] Owing to the metal-over-metal stacking fashion, a repulsive force works between the neighboring Ni atoms in $NiPc(AsF_6)_{0.5}$, whereas an attractive force works between the Co atoms in $CoPc(AsF_6)_{0.5}$. Probably for this reason, NiPc is stacked in a slightly zigzag fashion, and thus the symmetry of the molecular arrangement is lowered from tetragonal symmetry. The parameter *c* decreases systematically with the increase of *x*. This result shows that CoPc is mixed in the $NiPc(AsF_6)_{0.5}$ crystal lattice on a molecular level when $x=0.25$ and 0.45.

CCDC reference numbers 156502 and 156503. See http://www.rsc.org/suppdata/jm/b1/b100043h/ for crystallographic data in CIF or other electronic format.

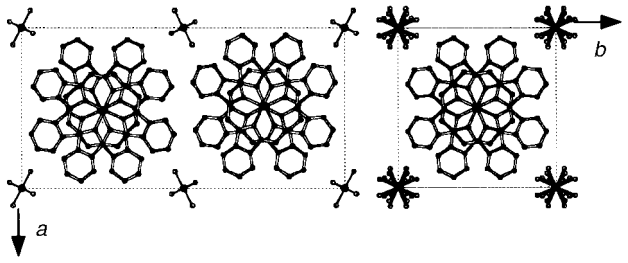

Fig. 1 Crystal structures of $Co_{0.25}Ni_{0.75}Pc(AsF_6)_{0.5}$ (left) and $Co_{0.45}Ni_{0.55}Pc(AsF_6)_{0.5}$ (right) viewed along the stacking direction. AsF_6^- in $Co_{0.45}Ni_{0.55}Pc(AsF_6)_{0.5}$ is orientationally disordered.

Magnetic properties

ESR signals were found in the alloy with $x \leqslant 0.09$. Fig. 2 shows the typical anisotropic hyperfine structures found in $Co_{0.01}Ni_{0.99}Pc(AsF_6)_{0.5}$ at 3.5 K ($H//c$) and 3.2 K ($H\perp c$). The *g* value is determined at the mid-field between $M_I=\pm 1/2$ lines. Since the molecules are arranged in a nearly tetragonal

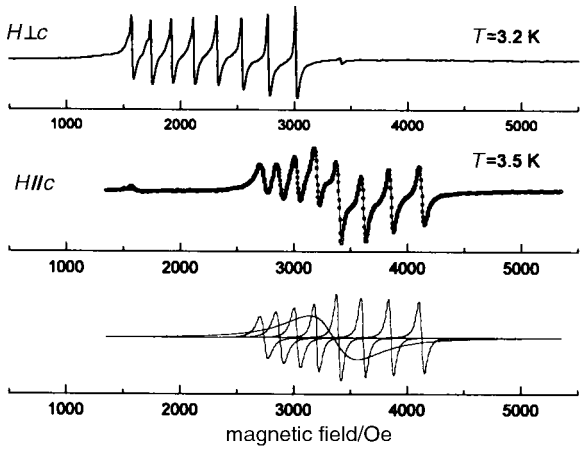

Fig. 2 Anisotropic hyperfine structure of the oriented single crystals of $Co_{0.01}Ni_{0.99}Pc(AsF_6)_{0.5}$. The circles in the $H//c$ spectrum represent the experimental data, and the solid line is the least-squares-fit curve composed of 8 sharp and 1 broad Lorentzians. Each Lorentzian is drawn at the bottom of this figure.

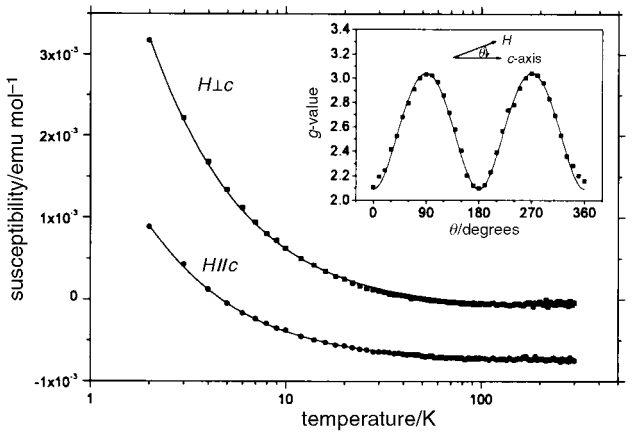

Fig. 3 Temperature dependence of the magnetic susceptibility of $Co_{0.01}Ni_{0.99}Pc(AsF_6)_{0.5}$. The diamagnetic contribution is not subtracted. The solid lines are the best-fit curves of a Curie–Weiss model. The inset shows the angular dependence of the g value of $Co_{0.01}Ni_{0.99}Pc(AsF_6)_{0.5}$.

fashion, the angular dependence of the g value is expected to conform to the following equation, if CoPc is relevantly substituted in the crystal lattice of $NiPc(AsF_6)_{0.5}$,

$$g(\theta)=(g_{//}^2\cos^2\theta+g_{\perp}^2\sin^2\theta)^{1/2} \quad (1)$$

where θ is the angle between the c-axis and magnetic field, and $g_{//}$ and $g_{\perp}$ are the principal g values parallel and perpendicular to the c-axis, respectively. As shown in the inset of Fig. 3, the g value of the 3.2 K signal exactly follows eqn. (1). The separation between the hyperfine lines significantly increases toward higher fields. This hyperfine structure is analyzed according to the Hamiltonian in the field of axial symmetry,[13] which is used for the analysis of the ESR signal of the magnetically diluted CoPc.[14] The anisotropic g values and hyperfine constants A (//) and B ($\perp$) are shown in Table 2 along with those of CoPc diluted in the insulating β-NiPc and α-ZnPc crystals. The hyperfine constants of the Co^{2+} ion in $Co_{0.01}Ni_{0.99}Pc(AsF_6)_{0.5}$ resemble those in β-$Co_{0.001}Ni_{0.999}Pc$ rather than in α-$Co_{0.001}Zn_{0.999}Pc$. This is because the local environment of the Co^{2+} ion doped in $NiPc(AsF_6)_{0.5}$ resembles that in β-NiPc.[14] The resemblance of the anisotropic g values as well as the anisotropic hyperfine constants to the magnetically diluted CoPc in β-NiPc indicates that the ESR signal of this compound is coming from the $CoPc^0$ substituted in the molecular column of $NiPc^{0.5+}$. No super-hyperfine structure from the nearest four nitrogen atoms is observed in $Co_{0.01}Ni_{0.99}Pc(AsF_6)_{0.5}$ or in magnetically diluted CoPc in α-ZnPc and β-NiPc. This result indicates that the unpaired electron occupies the $3d_{z^2}$ orbital of Co^{2+}, and this orbital is not extended to the nitrogen atoms.[15] The very anisotropic g value also supports the $3d_{z^2}$ orbital for the location of the unpaired electron in CoPc.[16]

As shown in Fig. 2, the $H//c$ signal is well reproduced by the superposition of the sharp hyperfine signals and a broad one with a linewidth of 420 G. The integrated intensities of the sum of the sharp signals and broad signal are 15% and 85%, respectively. The sharp signals are ascribed to free CoPc

Table 2 Anisotropic g values and hyperfine constants

Material	Temperature/K	$g_{//}$	$g_{\perp}$	A/cm^{-1}	B/cm^{-1}
$Co_{0.01}Ni_{0.99}Pc(AsF_6)_{0.5}$	3.2, 3.5	2.056(4)	3.045(4)	0.019(1)	0.029(1)
β-$Co_{0.001}Ni_{0.999}Pc$[a]	77, 27	1.89(1)	2.94(1)	0.015(1)	0.028(1)
α-$Co_{0.001}Zn_{0.999}Pc$[a]	300, 77, 27	2.007(3)	2.422(3)	0.0116(3)	0.0066(3)

[a]These data are taken from ref. 14.

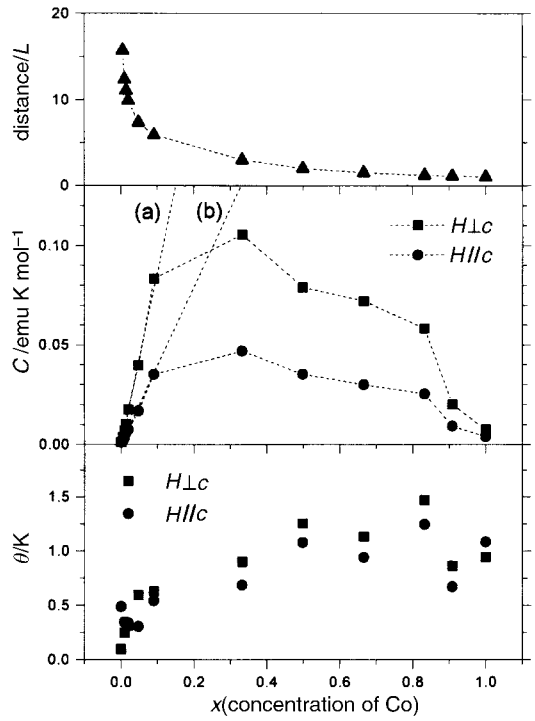

Fig. 4 Concentration (x) dependence of Curie constant and average distances between the doped CoPc molecules within the same molecular stack of $Co_xNi_{1-x}Pc(AsF_6)_{0.5}$. See the text for the description of the straight lines (a) and (b).

isolated from other CoPc and the broad one to relatively close CoPc, the signal of which is broadened by the dipole–dipole interaction. The ESR signal ascribed to isolated $CoPc^+$ is not found. Very similar hyperfine signals were observed in the mixed crystals with $x=0.005$, 0.014, 0.02, and 0.05. When the CoPc content is increased, the contribution of the broad signal increases, and the signal of $Co_{0.09}Ni_{0.91}Pc(AsF_6)_{0.5}$ ($x=0.09$) becomes nearly a single peak with a linewidth of *ca.* 500 G. No ESR signal was observed in the alloy with $x>0.1$. This tendency is reasonable, since the probability of close CoPc quickly increases when x increases. We examined the angular dependence of the g values in all these alloys. Every signal with $x\leqslant 0.09$ follows eqn. (1). This means that CoPc is microscopically substituted in $NiPc(AsF_6)_{0.5}$ at least in the range of $0.005\leqslant x\leqslant 0.09$.

Fig. 3 shows the static magnetic susceptibility of $Co_{0.01}Ni_{0.99}Pc(AsF_6)_{0.5}$. As shown in this figure, the susceptibility consists of Curie–Weiss and temperature-independent terms. The observed susceptibility is fitted very well by the equation, $\chi_{\perp,//}(T)=C_{\perp,//}/(T-\theta_{\perp,//})+\chi_{0\perp,//}$ down to 2 K, where $\perp$ and // represent the magnetic field perpendicular and parallel to the c-axis. The Curie constant and Weiss temperature in $Co_{0.01}Ni_{0.99}Pc(AsF_6)_{0.5}$ are determined as $C_{\perp}=0.0075$ emu K mol^{-1}, $\theta_{\perp}=-0.25$ K, $C_{//}=0.0038$ emu K mol^{-1}, and $\theta_{//}=-0.28$ K. The ratio of the Curie constants $C_{\perp}/C_{//}$ is a little smaller than $(g_{\perp}/g_{//})^2$. This is ascribed to a paramagnetic defect or impurity with an isotropic g value of 2.0023 in $NiPc(AsF_6)_{0.5}$. Taking the contribution of isotropic species into account, we determined the concentrations of the paramagnetic species as 0.77% for doped CoPc and 0.21% for a defect. The concentration of CoPc agrees well with the dopant concentration (1%) in the starting material. Therefore both the sharp and broad signals contribute to the Curie constant, and thus the distance between the close CoPc molecules is long enough to avoid direct exchange interactions. When the concentration of CoPc is increased, the Curie constant linearly increases in the range of $0.005\leqslant x\leqslant 0.09$, and reaches a maximum around $x\approx 0.33$, and then decreases in the range of $0.5\leqslant x\leqslant 1$. The x dependences of the Curie constant (C) and Weiss temperature

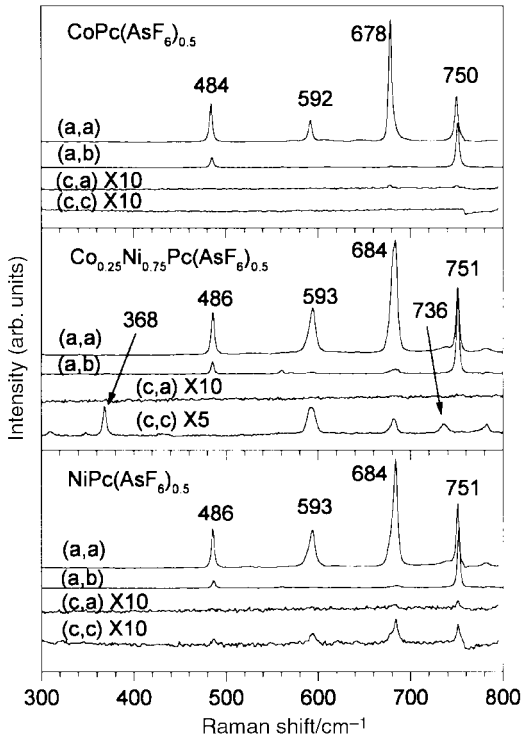

Fig. 5 Polarized Raman spectra of $Co_xNi_{1-x}Pc(AsF_6)_{0.5}$ ($x=0$, 0.25, 1). Weak spectra in (c,a) and (c,c) polarization are magnified by 5 or 10 times. Note that two new bands indicated by arrows are found in the alloy crystals.

(θ) are shown in Fig. 4 together with the average distance (L) along the c-axis. The average distance measured by the unit of inter-molecular distance along the stack ($c/2$) is estimated from the equation, $(2a/c)^{2/3}x^{-1/3}$ for $0 \leqslant x < 0.2$ and x^{-1} for $0.2 < x \leqslant 0$ taking the disk-like molecular shape into account. The Curie constant linearly increases when the average distance is less than 6 molecules along the stack ($0 \leqslant x < 0.1$). The straight lines (a) and (b) represent $(N_A g_\perp{}^2 \mu_B{}^2 S(S+1)/3k_B)x$ ($g_\perp = 3.045$) and $(N_A g_{//}{}^2 \mu_B{}^2 S(S+1)/3k_B)x$ ($g_{//} = 2.056$), respectively. In this range, all the doped CoPc contributes to the Curie term in magnetic susceptibility, and thereby the magnetic moments of CoPc molecules are nearly free from each other. The strength of the antiferromagnetic interaction between the magnetic moments is reflected in θ.[17] In the range of $0 \leqslant x < 0.1$, θ increases with x below 0.75 K. Therefore the indirect Co–Co interaction *via* the conduction electrons in the Pc chain seems to be very weak.[7] When x is increased, the Curie constant reaches a maximum around $x = 0.33$ and decreases toward zero. This behavior is different from the cases of $Cu_xNi_{1-x}Pc(I_3)_{0.33}$ and $Cu_xH_{2(1-x)}Pc(I_3)_{0.33}$,[7] in which the Curie constants linearly increase in the whole range of $0 \leqslant x \leqslant 1$. The different x dependence of the Curie constant is attributed to the different SOMO, which is $3d_{z^2}$ in CoPc and is $3d_{x^2-y^2}$ in CuPc. The former is extended to the neighbor Co^{2+} in CoPc, whereas the latter is elongated to the four nitrogen atoms in the Pc plane. With increasing x, the average distance between CoPc in the stacking direction becomes short. When $x = 0.33$, for example, L is about 2. As a result, there exists a considerable number of CoPc pairs in the same stack, which form a spin singlet. Therefore, the decrease of the Curie term in $x \geqslant 0.33$ is caused by direct antiferromagnetic interaction, since the probability of finding the CoPc in a neighboring position along the stack becomes higher. In $CoPc(AsF_6)_{0.5}$ ($x=1$), the Curie term is almost completely suppressed except for the small Curie component coming from a small amount of crystal defect. This result means that the 3d-orbital overlap between the neighboring molecules is extremely small in $CuPc(I_3)_{0.33}$ but significantly large in $CoPc(AsF_6)_{0.5}$.

Polarized Raman spectrum

We have compared the Raman spectra of CoPc and NiPc with those of the corresponding charge-transfer salts $CoPc(AsF_6)_{0.5}$ and $NiPc(AsF_6)_{0.5}$ in the region of 150–2000 cm^{-1}. The frequency shift caused by partial oxidation is less than 6 cm^{-1}, which is much smaller than the oxidation shift found in organic conductors such as $(BEDO\text{-}TTF)_2X$.[18] Since $CoPc(AsF_6)_{0.5}$ has high symmetry, D_{4h}, the polarized Raman spectrum of this compound provides information on the symmetry of the molecular vibrations. The normal modes of the free CoPc molecule are classified into the following representation:

$$\Gamma_{vib} = 14a_{1g} + 13a_{2g} + 14b_{1g} + 14b_{2g} + 13e_g + 6a_{1u} + 8a_{2u} + 7b_{1u} + 7b_{2u} + 28e_u$$

The symmetry of the coupled vibrations in the unit cell is connected with that of the free molecule by means of factor group analysis as shown in Table 3. The polarized Raman spectrum of $CoPc(AsF_6)_{0.5}$ is shown in the top panel of Fig. 5. The four strong bands at 484, 592, 678, and 750 cm^{-1} in (a,a) polarization have been respectively assigned to a_{2g}, b_{2g}, a_{1g}, and b_{1g} modes by Bartholomew *et al.*[19] According to Table 3, A_{1g} and B_{1g} modes are Raman active in (a,a) polarization, and these modes are derived from a_{1g}, a_{2g}, b_{1g}, and b_{2g} molecular vibrations.[20] Thus the result of the (a,a) spectrum is consistent with that described in ref. 18. In (a,b) polarization, the Raman active modes are assigned to B_{2g} symmetry derived from the b_{1g} or b_{2g} molecular vibrations. Therefore, the a_{1g} and a_{2g} molecular vibrations should disappear in (a,b) polarization compared with the observed modes in (a,a) polarization. As shown in Fig. 5, the 592 and 678 cm^{-1} bands disappear in (a,b) polarization, and thus these two bands can be assigned to the a_{1g} or a_{2g} mode. For the same reason, the symmetry of the 484 and 750 cm^{-1} bands is assigned to b_{1g} or b_{2g}. As shown above, the polarization dependence indicates that the symmetry of the 484 and 592 cm^{-1} bands is different from the assignment of ref. 18. The symmetry of these bands should be corrected as b_{1g} or b_{2g} for 484 cm^{-1} and a_{1g} or a_{2g} for 592 cm^{-1}. No Raman-active band was found in (c,a) polarization. This is reasonable because only the E_g mode, which is an out-of-plane vibration, is allowed in this polarization. The spectrum in (c,c) polarization is also very weak, since this polarization is associated with the Raman tensor of $d\alpha_{cc}/dQ$, which is the tensor component perpendicular to the molecular plane. The result of $NiPc(AsF_6)_{0.5}$ shown in the bottom panel is nearly the same as that of $CoPc(AsF_6)_{0.5}$. Although the molecular arrangement is approximately the same as $CoPc(AsF_6)_{0.5}$, the crystal symmetry is lower than $CoPc(AsF_6)_{0.5}$. As a result, the above four bands weakly appear in the (c,c) spectrum.

The Raman spectra of $Co_xNi_{1-x}Pc(AsF_6)_{0.5}$ in (a,a)

Table 3 Correlation diagram in $CoPc(AsF_6)_{0.5}$

Molecule D_{4h}	Site C_{4h}	Unit cell D_{4h} ($Z=2$)	Selection rules
14 a_{1g} (in-plane) 13 a_{2g} (in-plane)	27 A_g	27 A_{1g} (in-phase) 27 A_{2g} (out-of-phase)	$\alpha_{xx}+\alpha_{yy}$, α_{zz}
14 b_{1g} (in-plane) 14 b_{2g} (in-plane)	28 B_g	28 B_{1g} (in-phase) 28 B_{2g} (out-of-phase)	$\alpha_{xx}-\alpha_{yy}$ α_{xy}
13 e_g (out-of-plane)	13 E_g	26 E_g	α_{xz}, α_{yz}
6 a_{1u} (out-of-plane) 8 a_{2u} (out-of-plane)	14 A_{1u}	14 A_{1u} (in-phase) 14 A_{2u} (out-of-phase)	T_z
7 b_{1u} (out-of-plane) 7 b_{2u} (out-of-plane)	14 B_{1u}	14 B_{1u} (in-phase) 14 B_{2u} (out-of-phase)	
28 e_u (in-plane)	28 E_u	28 E_u	T_x, T_y

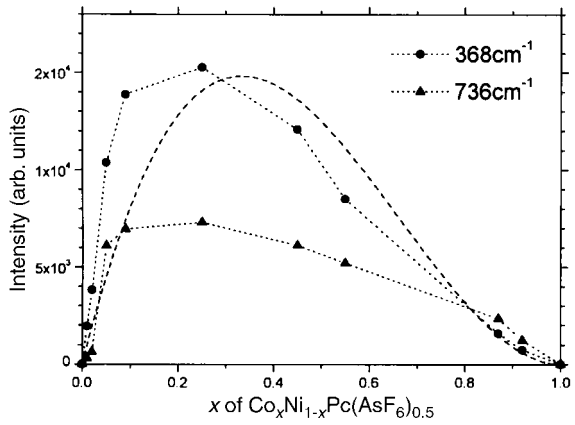

Fig. 6 The intensities of the new Raman bands observed in alloys are plotted against x of $Co_xNi_{1-x}Pc(AsF_6)_{0.5}$.

polarization consist of the superposition of the spectra of $CoPc(AsF_6)_{0.5}$ and $NiPc(AsF_6)_{0.5}$. However, in (c,c) polarization, new peaks are found at 368 cm^{-1} and 736 cm^{-1} in addition to the A_{1g} bands [see the bands indicated by arrows]. These new bands are observed neither in $CoPc(AsF_6)_{0.5}$ nor in $NiPc(AsF_6)_{0.5}$ but are found in all alloys, and observed only in (c,c) polarization. This polarization dependence indicates that the 368 cm^{-1} and 736 cm^{-1} bands are the a_{1g} or a_{2g} in-plane molecular vibrations. It is surprising that these Raman bands are observable even in a dilute alloy $Co_{0.01}Ni_{0.99}Pc(AsF_6)_{0.5}$. The 736 cm^{-1} band is regarded as the second harmonic band of 368 cm^{-1}. Furthermore, these new Raman bands were suppressed when an Ar^+ laser (515 nm) was used as an excitation source. We therefore consider that these two bands are enhanced by a resonance effect *via* the newly formed excited state in the alloy and thus belong to the a_{1g} symmetry. The optical transition to the new excited state at $\sim$2 eV should be polarized along the conducting axis (*c*-axis). Accordingly, this optical transition can be ascribed to the inter-molecular charge-transfer transition between CoPc and NiPc. We measured the *E*//*c* polarized reflectivity of $Co_xNi_{1-x}Pc(AsF_6)_{0.5}$ in the region of 1.3–4.1 eV. The *E*//*c* reflectivity in this spectral region is less than 3% and has almost no structure. More exactly, a very weak and broad hump is found at 1.8–2.3 eV in the crystals with $x=0.25$, 0.45, and 0.55. In this spectral region, there is an allowed optical transition (Q-band) from HOMO (a_{1u}) to LUMO (e_g) polarized parallel to the *a* and *b*-axes. The vacant $3d_{x^2-y^2}$ orbital (b_{1g}) is located near LUMO (e_g) and occupied $3d_{z^2}$ is near HOMO (a_{1u}), according to the molecular orbital calculation.[21] Thus, the energy difference between the $3d_{x^2-y^2}$ and $3d_{z^2}$ orbitals is considered to be $\sim$2 eV. We therefore propose that the new optical transition produced in the alloy system is associated with the inter-molecular charge-transfer transition between the $3d_{z^2}$ orbital (a_{1g}) and $3d_{x^2-y^2}$ orbital (b_{1g}). This charge-transfer transition is forbidden when the molecules are arranged in a tetragonal system. This property is consistent with the extremely weak dispersion in the reflectivity and the rather weak intensity for a resonance-enhanced Raman mode. According to the normal coordinate analysis of porphyrins,[22,23] the $\sim$350 cm^{-1} band is assigned to the breathing mode (a_{1g}) of the macrocycle around the central metal. We therefore assign the 368 cm^{-1} and 736 cm^{-1} bands to the a_{1g} breathing mode and its second harmonic mode. Fig. 6 shows the x dependence of the intensities of the 368 cm^{-1} and 736 cm^{-1} bands. These bands appear more strongly in $x<0.5$ than in $x>0.5$. The probability of finding NiPc and CoPc in the neighboring position in $Co_xNi_{1-x}Pc(AsF_6)_{0.5}$ is $x(1-x)$, which is a symmetric function with respect to $x=0.5$. If we assign the 368 cm^{-1} band to the breathing mode of NiPc, the intensity is proportional to $x(1-x)^2$, which qualitatively reproduces the x dependence of the Raman intensity shown in Fig. 6.[24] Therefore, a plausible assignment for the optical transition is described by the following scheme:

$$Co(3d_{z^2})^1(3d_{x^2-y^2})^0Ni(3d_{z^2})^2(3d_{x^2-y^2})^0 \rightarrow$$
$$Co(3d_{z^2})^0(3d_{x^2-y^2})^0Ni(3d_{z^2})^2(3d_{x^2-y^2})^1$$

Finally it should be noted that the observation of the new Raman bands is strong evidence for the formation of the alloy in a wide range of x.

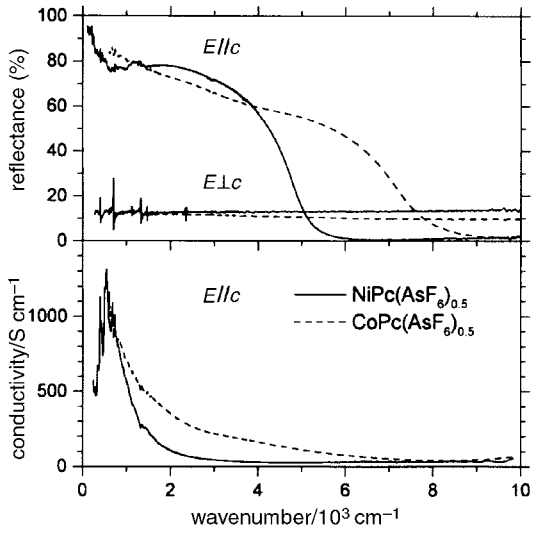

Fig. 7 Polarized reflection spectra of $NiPc(AsF_6)_{0.5}$ (solid line) and $CoPc(AsF_6)_{0.5}$ (broken line). The optical conductivity obtained *via* Kramers–Kronig transformation is drawn in the bottom panel.

Reflectivity

The reflectivity data in the low-frequency region provide information on the bandwidth and anisotropy of a conduction band. Fig. 7 shows the reflection spectra of $NiPc(AsF_6)_{0.5}$ and $CoPc(AsF_6)_{0.5}$. It is obvious from the polarization of the reflectivity that both compounds have a quasi-1D band along the *c*-axis. In both compounds, the macrocycles (Pc) are oxidized by half, so Pc forms a $\frac{3}{4}$-filled quasi-1D band (π band). Although the crystal structure of $CoPc(AsF_6)_{0.5}$ is nearly the same as $NiPc(AsF_6)_{0.5}$, the reflectivity is very different. In $NiPc(AsF_6)_{0.5}$, the high-frequency part of the reflectivity can be fitted well by a Drude model. Owing to the broad dip at $\sim$600 cm^{-1}, the optical conductivity exhibits a peak at this spectral region as shown in the bottom panel of Fig. 7. Although the origin of the broad dip around 600 cm^{-1} is not clear at the moment, we consider that this is associated with the correlation gap which is found in highly correlated quasi-1D organic metals such as $(TMTSF)_2X$.[25] On the other hand, the reflectivity of $CoPc(AsF_6)_{0.5}$ in the low-frequency region appears to be Drude-like down to 600 cm^{-1} but the reflectivity in the mid-infrared region cannot be reproduced by a Drude model.[26] To reproduce the reflectivity curve, a Lorentz oscillator is necessary at $\sim$4000 cm^{-1} in addition to the Drude term. The increase of the spectral weight in the mid-infrared region of the optical conductivity is shown in the bottom panel of Fig. 7.

We analyzed the reflection spectra using the following Drude and Lorentz models,

$$\varepsilon(\omega)=\varepsilon_\infty-\frac{\omega_p^2}{\omega(\omega+i\gamma)}+\frac{\Omega_p^2}{\Omega_0^2-\omega^2-i\omega\Gamma}$$

The fitting parameters for the Drude and Lorentz functions are shown in Table 4. The total plasma frequency defined by

Table 4 Parameters of Drude and Lorentz functions

	ε_∞	ω_p/ 10^3 cm^{-1}	γ/ 10^3 cm^{-1}	Ω_p/ 10^3 cm^{-1}	Ω_0/ 10^3 cm^{-1}	Γ/ 10^3 cm^{-1}
NiPc-$(AsF_6)_{0.5}$	2.39	4.29	0.17	6.23	0.74	1.05
CoPc-$(AsF_6)_{0.5}$	3.31	12.8	1.49	4.51	3.90	2.78

$\Omega_p{}^T=(\omega_p{}^T+\Omega_p{}^T)^{1/2}$ is associated with the transition probability of the optical transition in this spectral region. If the spectrum consists of a single component, the oscillator strength of this optical transition is determined by the overlap integral of the a_{1u} HOMOs of the macrocycle (Pc) between the nearest neighbor molecules. The ratio of the square total plasma frequency $(\Omega_p{}^T(\mathrm{Co})/\Omega_p{}^T(\mathrm{Ni}))^2=3.2$ is too large to be regarded as a single component. This large ratio strongly suggests that the 3d orbital also contributes to the optical transition of $CoPc(AsF_6)_{0.5}$ in the mid-infrared region. As described in the section describing magnetic properties, the singly occupied $3d_{z^2}$ orbital is extended to the neighbor molecules. Therefore the $3d_{z^2}$ orbital forms a half-filled 1D band ($3d_{z^2}$ band) along the Co chain. It is well-known that a half-filled 1D band is split into upper and lower Hubbard bands, if we take the on-site Coulomb interaction into account. The optical transition between these split bands is polarized along the Co chain direction (*c*-axis). Therefore, it is reasonable to assign the mid-infrared band at $\sim$0.5 eV to this optical transition. The excitation energy of this transition is comparable with that of a half-filled quasi-1D π electron system such as LiPc.[27] This small excitation energy is surprising, because the excitation energy or the gap between the split bands is associated with the on-site Coulomb energy. In the Co chain, the electrons in the $3d_{z^2}$ band are confined within a narrow space, whereas the electrons in the π band are more extended in large Pc. Thus the on-site Coulomb energy in the $3d_{z^2}$ band seems to be much larger than that in the π band. For example, the on-site Coulomb energy is estimated as $\sim$5 eV in the 1D Ni complexes.[28] The remarkable reduction of the on-site Coulomb energy in $CoPc(AsF_6)_{0.5}$ is probably caused by the strong polarization effect by the conjugated π-electron in the macrocycle surrounding the Co chain along the *c*-axis. In this system, the macrocycle (Pc) contributes to the intra- and inter-molecular polarization effects. As the metallic π electrons are highly polarizable, we consider that the inter-molecular polarization effect is dominant in this compound.

Let us briefly compare the reflectivity of $CoPc(AsF_6)_{0.5}$ with that of $CuPc(I_3)_{0.33}$. The reflectivity in the infrared region has not been reported for the latter compound. According to the reflectivity observed down to 3500 cm^{-1}, the plasma edge appears at $\sim$4500 cm^{-1} with the plasma frequency of

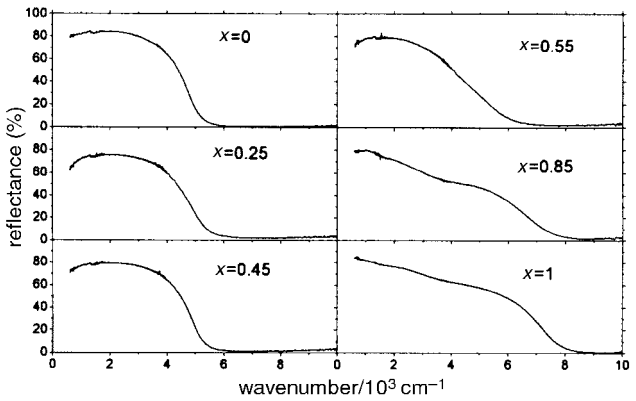

Fig. 8 Concentration (x) dependence of the reflectivity polarized parallel to the *c*-axis.

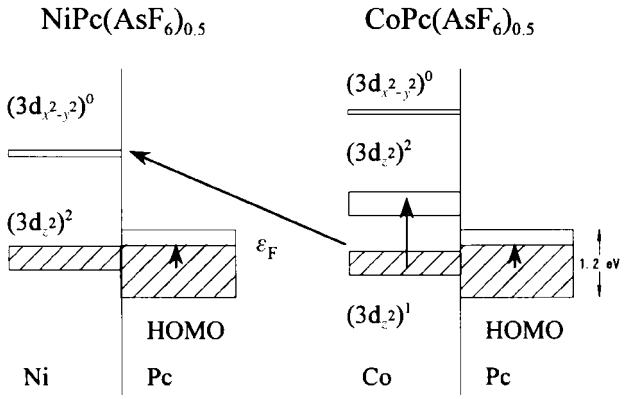

Fig. 9 Schematic energy diagrams of $NiPc(AsF_6)_{0.5}$ and $CoPc(AsF_6)_{0.5}$. The arrows denote the optical transitions polarized along the conducting axis found in this study.

6.7×10^3 cm^{-1}.[2] The plasma frequency is not close to that of $CoPc(AsF_6)_{0.5}$ but to $NiPc(AsF_6)_{0.5}$, although the 3d orbital of Cu^{2+} is singly occupied. This result suggests that the 3d orbital of Cu^{2+} does not contribute to the low-energy optical transition along the conducting axis. This suggestion is consistent with the extremely small orbital overlap between the nearest neighbor Cu–Cu, as described in the section of magnetic properties. Therefore the resemblance between $CuPc(I_3)_{0.33}$ and $NiPc(AsF_6)_{0.5}$ is reasonable. This comparison also supports the interpretation that the $3d_{z^2}$ orbital contributes to the low-energy optical transition in $CoPc(AsF_6)_{0.5}$.

Fig. 8 shows the x dependence of the reflectivity polarized along the *c*-axis. In the range of $0\leqslant x\leqslant0.45$, the spectral shapes are essentially the same, except that the plasma edge slightly moves to the high-frequency side. This means that the center energy of the π band of $NiPc(AsF_6)_{0.5}$ nearly coincides with that of $CoPc(AsF_6)_{0.5}$. The x dependence of the reflectivity is not a weighted average. The characteristic line shape of $CoPc(AsF_6)_{0.5}$ is observed only in the region of $0.87\leqslant x\leqslant1$, which is closer to $x=1$. This spectral dependence is consistent with our interpretation that the optical transition in the mid-infrared region is assignable to the inter-molecular charge-transfer transition along the Co chain that requires the CoPc pair. The probability to find the pair does not increase linearly but proportionally to x^2.

Finally, in Fig. 9 we show the schematic energy diagrams of $NiPc(AsF_6)_{0.5}$ and $CoPc(AsF_6)_{0.5}$. From the results shown in Fig. 8, the π bands are placed on the same energy level. We have examined the pressure dependence of the optical absorption of $NiPc(AsF_6)_{0.5}$ and $CoPc(AsF_6)_{0.5}$, and have clarified that the filled $3d_{z^2}$ band is located close to the Fermi level.[11] The difference between $NiPc(AsF_6)_{0.5}$ and $CoPc(AsF_6)_{0.5}$ is the energy level of the $3d_{z^2}$ band, that is, the $3d_{z^2}$ band of $CoPc(AsF_6)_{0.5}$ is a little higher than that of $NiPc(AsF_6)_{0.5}$. Therefore the lower Hubbard band ($(3d_{z^2})^1$ band) is located close to the Fermi level in $CoPc(AsF_6)_{0.5}$, whereas the upper Hubbard band ($(3d_{z^2})^2$ band) is close to the Fermi level in $NiPc(AsF_6)_{0.5}$. As a result, as shown by the arrows in Fig. 9, the *E*//*c* spectrum consists of two optical transitions (two components) in $CoPc(AsF_6)_{0.5}$ and one optical transition (single component) in $NiPc(AsF_6)_{0.5}$. The existence of a very weak band is deduced from the Raman spectrum of the alloy, $Co_xNi_{1-x}Pc(AsF_6)_{0.5}$. This inter-molecular charge-transfer transition is denoted by the long arrow. This energy diagram explains the nearly temperature-independent paramagnetic term in the magnetic susceptibility. The corresponding values for powdered samples are $(4–5)\times10^{-4}$ emu mol^{-1} for $CoPc(AsF_6)_{0.5}$ and $(0.5–1)\times10^{-4}$ emu mol^{-1} for $NiPc(AsF_6)_{0.5}$. The enhanced paramagnetic susceptibility in $CoPc(AsF_6)_{0.5}$ is ascribed to the highly correlated 1D $3d_{z^2}$ band.

Summary

Organic alloys $Co_xNi_{1-x}Pc(AsF_6)_{0.5}$ were prepared for the whole range of x between 0 and 1. X-Ray diffraction, ESR, and Raman spectra indicated that CoPc and NiPc were mixed on a molecular level in these charge-transfer salts. In particular, in the range of $0 \leqslant x \leqslant 0.09$, the orientation of doped CoPc and SOMO of CoPc were well characterized by the hyperfine structure in the ESR experiment. In the Raman spectra of alloys, we found new vibrational bands enhanced by resonance effects, and pointed out the existence of a very weak optical transition polarized at ~ 2 eV along the c-axis. Based on the analysis of the low-energy reflectivity, we conclude that the $3d_{z^2}$ orbital forms a half-filled 1D band, which is split into a filled lower band and a vacant upper band, owing to the on-site Coulomb energy. The difference in magnetic and optical properties between $NiPc(AsF_6)_{0.5}$ and $CoPc(AsF_6)_{0.5}$ is attributed to the different energy levels of the $3d_{z^2}$ orbitals.

Acknowledgements

This research was supported in part by a Grant-in-Aid for Scientific Research on Priority Areas (B) of Molecular Conductors and Magnets (Area No. 730/Grant No. 11224212) from the Ministry of Education, Science, Sports, and Culture of Japan.

References

1 M. Y. Ogawa, B. M. Hoffman, S. Lee, M. Yudkowski and W. P. Halperin, *Phys. Rev. Lett.*, 1986, **57**, 1177.
2 M. Y. Ogawa, J. Martinsen, S. M. Palmer, J. L. Stanton, J. Tanaka, R. L. Green, B. M. Hoffman and J. A. Ibers, *J. Am. Chem. Soc.*, 1987, **109**, 1115.
3 G. Quirion, M. Poirier, K. K. Liou, M. Y. Ogawa and B. M. Hoffman, *Phys. Rev. B*, 1988, **37**, 4272.
4 G. Quirion, M. Poirier, C. Ayache, K. K. Liou and B. M. Hoffman, *J. Phys. I France*, 1992, **2**, 741.
5 M. Y. Ogawa, S. M. Palmer, K. K. Liou, G. Quirion, J. A. Thompson, M. Poirier and B. M. Hoffman, *Phys. Rev. B*, 1989, **39**, 10682.
6 G. Quirion, M. Poirier, K. K. Liou and B. M. Hoffman, *Phys. Rev. B*, 1991, **43**, 860.
7 J. Thompson, K. Murata, R. Durcharne, M. Poirier and B. M. Hoffman, *Phys. Rev. B*, 1999, **60**, 523.
8 J. Martinsen, J. L. Stanton, R. L. Green, J. Tanaka, B. M. Hoffman and J. A. Ibers, *J. Am. Chem. Soc.*, 1985, **107**, 6915.
9 K. Yakushi, H. Yamakado, T. Ida and A. Ugawa, *Solid State Commun.*, 1991, **78**, 919.
10 H. Yamakado, T. Ida, A. Ugawa, K. Yakushi, K. Awaga, Y. Maruyama, K. Imaeda and H. Inokuchi, *Synth. Met.*, 1994, **62**, 169.
11 T. Hiejima and K. Yakushi, *J. Chem. Phys.*, 1995, **103**, 3950.
12 K. Yakushi, H. Yamakado, M. Yoshitake, N. Kosugi, H. Kuroda, T. Sugano, M. Kinoshita, A. Kawamoto and J. Tanaka, *Bull. Chem. Soc. Jpn.*, 1989, **62**, 687.
13 B. Bleany, *Philos. Mag.*, 1951, **42**, 441.
14 J. M. Assour and W. K. Kahn, *J. Am. Chem. Soc.*, 1965, **87**, 207.
15 B. A. Goodman and J. B. Paynon, *Adv. Inorg. Chem. Radiochem.*, 1972, **13**, 135.
16 Y. Nishida and S. Kida, *Inorg. Nucl. Chem. Lett.*, 1971, **7**, 325.
17 I. Martin and P. Phillips, *Phys. Rev. B*, 1999, **60**, 530.
18 O. Drozdova, H. Yamochi, K. Yakushi, M. Uruichi, S. Horiuchi and G. Saito, *J. Am. Chem. Soc.*, 2000, **112**, 4436.
19 C. R. Bartholomew, A. A. McConnell and W. E. Smith, *J. Raman Spectrosc.*, 1989, **20**, 595.
20 The a_{2g} symmetry is inactive in normal Raman scattering. However, it is well known in porphyrins and phthalocyanines that the a_{2g} mode is allowed in the resonance region. T. G. Spiro and T. C. Strekas, *J. Am. Chem. Soc.*, 1974, **96**, 338.
21 F. W. Kutzler and E. E. Ellis, *J. Chem. Phys.*, 1986, **84**, 1033.
22 X.-Y. Li, R. S. Czernuszewicz, J. R. Kincaid, Y. O. Su and T. G. Spiro, *J. Phys. Chem.*, 1990, **94**, 31.
23 X.-Y. Li, R. S. Czernuszewicz, J. R. Kincaid, P. Stein and T. G. Spiro, *J. Phys. Chem.*, 1990, **94**, 47.
24 When we take the anisotropic unit cell into account, the corresponding function is given by $f(x)=(1-x^{1/3}(2a/c)^{2/3})x(1-x)$ in the range of $0 \leqslant x < 0.2$. However, the difference from the function $f(x)=x(1-x)^2$ is negligible for the qualitative discussion.
25 V. Vescoli, L. Degiorgi, W. Henderson, G. Gruner, K. P. Starkey and L. K. Montgomery, *Science*, 1998, **281**, 1181.
26 We could not measure the reflectivity of $CoPc(AsF_6)_{0.5}$ in the far-infrared region, since large single crystals could not be obtained.
27 K. Yakushi, T. Ida, A. Ugawa, H. Yamakado, H. Ishii and H. Kuroda, *J. Phys. Chem.*, 1991, **95**, 7636–7641.
28 H. Okamoto, Y. Shimoda, Y. Oka, A. Chainani, T. Takahashi, H. Kitagawa, T. Mitani, K. Toriumi, K. Inoue, T. Manabe and M. Yamashita, *Phys. Rev. B*, 1966, **54**, 8434.